



## SEISMIC RESPONSE EVALUATION OF AN RC BEARING WALL BY DISPLACEMENT-BASED APPROACH

Chang-Hun HYUN<sup>1</sup>, Sanghyun CHOI<sup>2</sup>, Kang-Ryong CHOI<sup>3</sup>, Hyun-Mock SHIN<sup>4</sup>, Ji-Hong PARK<sup>5</sup>

### SUMMARY

In this paper, the displacement-based seismic design approaches are evaluated utilizing shaking-table test data of a 1:3 scaled reinforced concrete bearing wall structure subjected to far- and near- field earthquake motions, provided by the International Atomic Energy Agency. The maximum responses such as the top displacement and base shear forces are estimated using the two prominent displacement-based approaches, i.e., the capacity spectrum method (ACT-40) and the displacement coefficient method (FEMA-356), and compared with the measured responses. For comparison purpose, conventional response spectrum analysis and nonlinear time history analysis are also performed. The results indicate that the capacity spectrum method underestimates the response of the structure in inelastic range while the displacement coefficient method yields reasonable values in most cases.

### INTRODUCTION

The usual engineering practices in seismic design of nuclear facilities result in a poor estimate of safety implications of near field earthquakes. Recent developments in earthquake engineering for non-nuclear facilities provide tools to cope with this difficulty. To determine to what extent these developments such as the displacement-based approaches can be recommended for the assessment of nuclear facilities subjected to near-field earthquake inputs, the International Atomic Energy Agency (IAEA) has initiated the Coordinated Research Program (CRP) on Safety Significance of Near Field Earthquake. As a first step of the program, five data sets of input excitations and measured responses were provided from the shaking-table test of a 1:3 scaled reinforced concrete (RC) bearing wall structure (CAMUS specimen) subjected to far- and near-field earthquake motions [1].

In this paper, the displacement-based seismic design approaches are evaluated utilizing the RC bearing wall experimental data. The test structure is modeled in two ways: a linear model using

---

<sup>1</sup> Principal Research Engineer, Korea Institute of Nuclear Safety, Deajeon, Korea. Email: k203hch@kins.re.kr

<sup>2</sup> Senior Research Engineer, Korea Institute of Nuclear Safety, Deajeon, Korea.

<sup>3</sup> Principal Research Engineer, General Manager, Korea Institute of Nuclear Safety, Deajeon, Korea.

<sup>4</sup> Professor, Sungkyunkwan Univ., Suwon, Korea. Email: hmshin@nature.skku.ac.kr

<sup>5</sup> Graduate Student, Sungkyunkwan Univ., Suwon, Korea.

beam elements and a nonlinear model using shell elements to assess linear and nonlinear responses, respectively. Linear and nonlinear static and dynamic analyses are performed using SAP2000<sup>®</sup> [2] and RCAHEST [3]. The maximum displacement and base shear forces are also estimated using the two prominent displacement-based approaches, i.e., the capacity spectrum method (ACT-40) [4] and the displacement coefficient method (FEMA-356) [5], and compared with the measured responses. For comparison purpose, conventional response spectrum analysis and nonlinear time history analysis are also performed.

### DESCRIPTION OF THE TEST

The 1:3 scaled test structure (CAMUS specimen) is composed of two parallel 5-floor RC walls without opening (Fig. 1) linked by 6 square floors [1]. The stiffness and the strength in the perpendicular direction (to the walls) are increased by adding lateral triangular bracings. Lateral bracings are such that the two walls carry the entire vertical load. The total height of the test structure is 5.10 m, and the width and thickness of each wall are 1.70 m and 6.0 cm, respectively. The total mass of the structure is estimated at about 36 tons. The mass of each floor without considering the additional masses is about 1.3 tons and the additional masses have been determined in order to impose a normal force to the walls compatible with the vertical stress values commonly found at the base of such structures (1.6 MPa in this case). The geometry of the floors with the additional masses can be seen in Fig. 2. The figure also gives the accumulated mass at each story (above and under the floor) for one wall. The position of each level in Fig. 2 is defined as the middle of the floor. The vertical stress just above the floor (i.e. at the level of the construction joint where cracking might occur) due to the dead load is also given in the figure. The steel reinforcement at each level is described in Fig. 2 as well.



Fig. 1. View of the RC wall structure

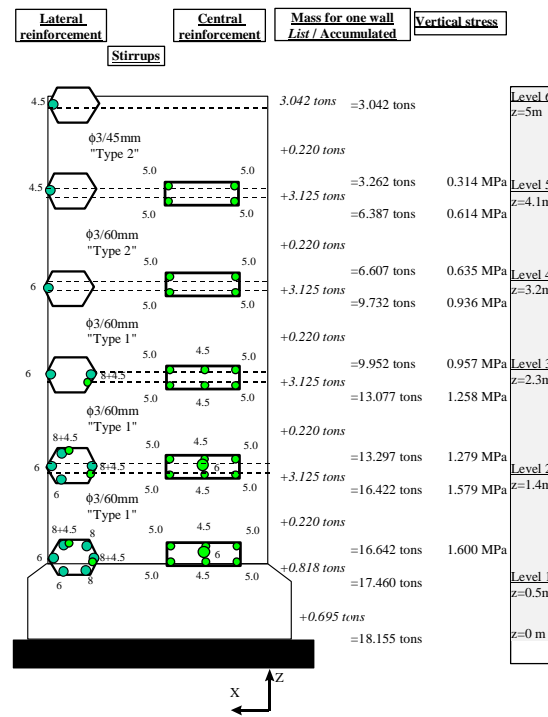


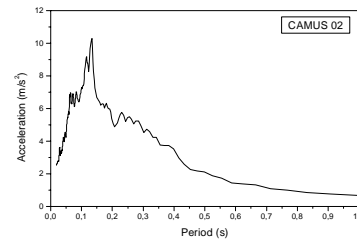
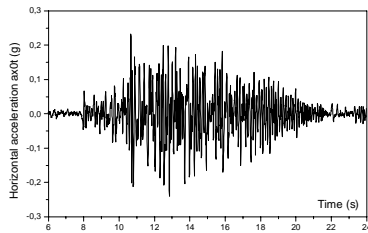
Fig. 2. Reinforcement and mass balance for one wall

Among the seismic excitations applied to the test structure, five seismic excitations in the direction of the wall are provided for this study. The maximum horizontal accelerations of the excitations are presented in Table 1 [1]. In the table, Runs 1, 4, and 5 (Nice input motion, artificial ground motion) represent far-field inputs and Runs 2 and 3 (San Francisco input motion, natural ground motion) represent near-field inputs. The input time histories and the corresponding response spectra are presented in Fig. 3.

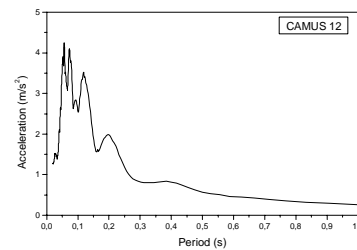
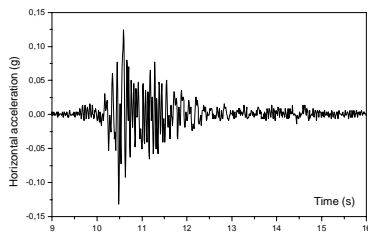
**Table 1. List of the seismic tests**

Tests	Run 1 <sup>(1)</sup>	Run 2 <sup>(2)</sup>	Run 3 <sup>(2)</sup>	Run 4 <sup>(1)</sup>	Run 5 <sup>(1)</sup>	Run 4-5 <sup>(3)</sup>
Maximum horizontal acceleration	0.24 g	0.13 g	1.11 g	0.41 g	0.72 g	0.41 g

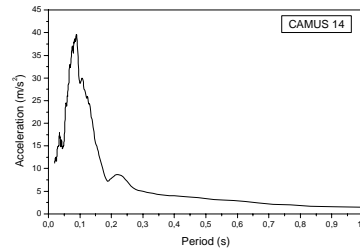
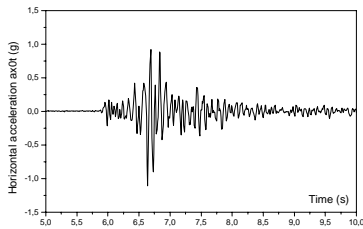
Note (1) Nice signal; (2) San Francisco signal; (3) Additional input motion defined in this study (scaled down from Run 5)



(a) Run 1

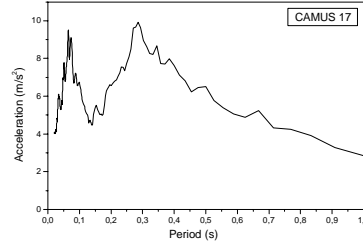
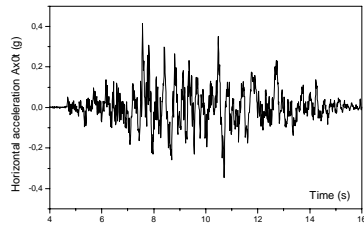


(b) Run 2

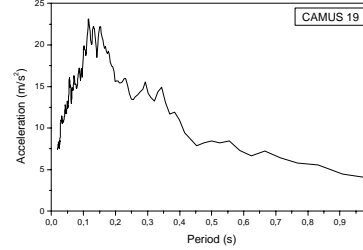
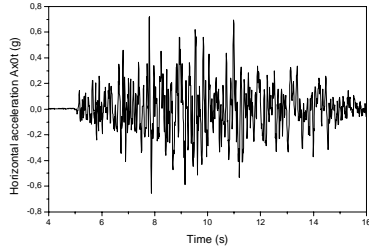


(c) Run 3

**Fig. 3. Input time histories and corresponding response spectra**



(d) Run 4



(e) Run 5

**Fig. 3. (continued) Input time histories and corresponding response spectra**

In the figure, one notable observation was made. Comparing Figs. 3(a), 3(d), and 3(e), it can be seen that Run 4 input motion is very different from Run 1 and Run 5 input motions, even though three motions are originated from the same Nice input motion. Preliminary nonlinear time history analysis (see the last Section) also indicates that the resulting response for Run 4 motion is significantly different from the test results. The authors conjectured that Run 4 motion might be a different motion from Nice motions. To verify the conjecture, nonlinear time history analysis was performed using the 0.41g (i.e., peak ground acceleration (PGA) of Run 4) input motion scaled down from Run 5 motion. As shown in the last Section, the results are in good agreement with the test results. The additional scaled-down input motion is designated as Run 4-5 in this study.

## FINITE ELEMENT MODELS

### Model for linear analysis

To investigate the effectiveness of typical linear seismic design practice, a linear model of the RC wall is developed using the commercial Finite Element (FE) analysis software, SAP2000<sup>®</sup> (1998). A schematic of the FE model is presented in Fig. 4. The linear model consists of six beam elements and a rotational and a translational spring at the support. The springs are used to reflect the effect of the vertical restraining rods of the shaking table. The beam is assumed to have the elastic modulus of 28,000 MPa. The translational and the rotational spring are assumed to have a modulus of 800 MN/m and 4,984 MN-m [1], respectively. Modal and response spectrum analyses were performed using the model.

### Model for nonlinear analysis

The nonlinear model of the RC wall is developed for one wall of the test model structure using the software RUAUMC developed by Kim and Shin [3]. The RC wall is modeled utilizing layered elements with 4-node plane shell elements for the concrete and the reinforcing bars. A total of 198 layered shell elements and 38 elastic (rigid) shell element are used for the RC wall and the shaking table, respectively.

Also, three translational spring elements with moduli of 200MN/m, 400MN/m and 200MN/m are used to simulate the vertical restraining rods of the shaking table. A schematic of the model is presented in Fig. 5.

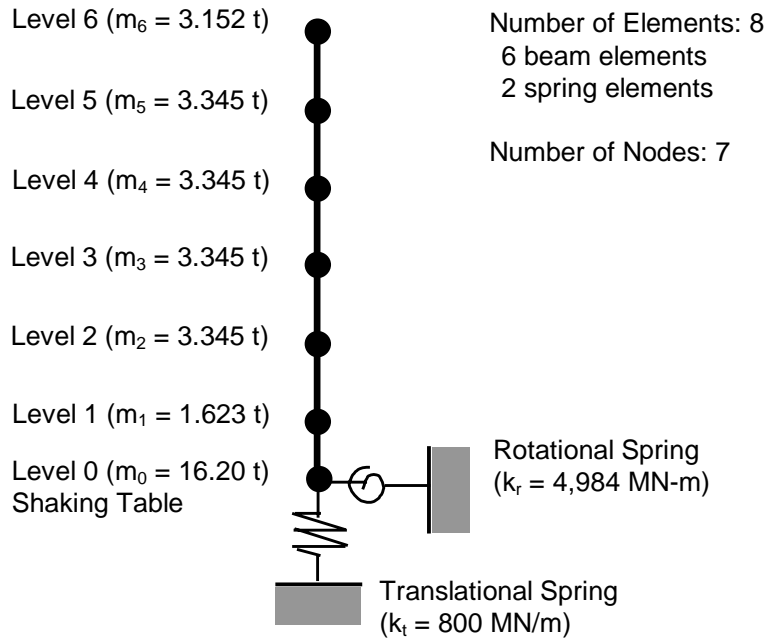


**Fig. 4. Schematic of the linear stick model for one wall**

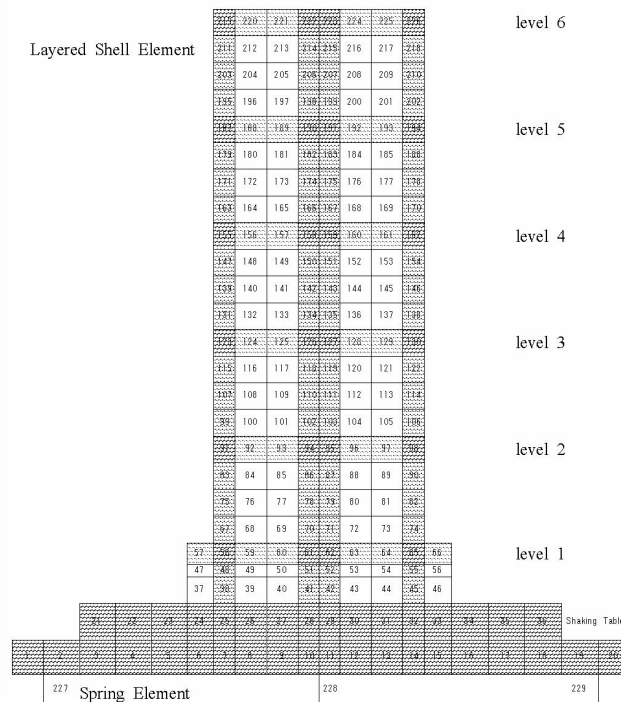


**Fig. 5. Schematic of the nonlinear analytical model**

The elasto-plastic and fracture model for the biaxial state of stress was used as a constitutive equation of uncracked concrete. The tension and the compression stiffness degradation models were used in the normal and the parallel directions to crack, and the shear transfer model was used in shear direction, to model the cracking behavior of the concrete in both tension and compression. In modeling the post-yield behavior of the reinforcing bar in concrete, the bond characteristics were taken into account. The material properties used in the model are summarized in Table 2. Nonlinear static and dynamic analysis were performed using the analytical model.

**Table 2. Material properties used in the RCAHEST model**

Concrete		Reinforcing bars	
Elastic Modulus	28,000 MPa	Elastic Modulus	200,000 MPa
Compressive Strength	30 MPa	Yield strength	500 MPa
Tensile Strength	2.6 MPa		
Poisson's Ratio	0.15		

### DISPLACEMENT-BASED APPROACHES

Two displacement-based nonlinear static procedures, i.e., the displacement coefficient method [5] and the capacity spectrum method [4], were used to estimate the maximum response of the structure. The methods can estimate the inelastic response of the structure without performing nonlinear dynamic analysis. Nonlinear static analyses were performed with the distributions of the lateral loads with an inverse triangular shape and proportional to the shape of fundamental mode by the following equation [4].

$$F_i = V \frac{m_i \phi_{1i}}{\sum_i m_i \phi_{1i}} \quad (1)$$

where  $F_i$  is the lateral load at the  $i^{\text{th}}$  floor;  $V$  is the base shear force;  $m_i$  is the mass of the  $i^{\text{th}}$  floor; and  $\phi_1$  is the fundamental mode shape of the elastic model of the structure. Presented in Fig. 6 is the applied lateral force distribution along with model height for the static analysis.

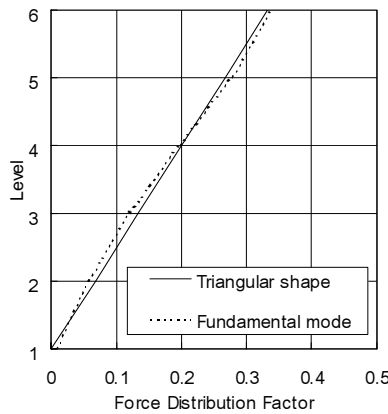


**Fig. 6. Applied lateral force distribution along with model height**

The pushover analysis is carried out by incrementally applying the lateral loads to the structure. The sequence of component cracking, yielding, and failure, as well as the history of deformations and shears in the structure, can be traced as the lateral loads are monotonically increased. The nonlinear analytical model was used to obtain the force-displacement curve (i.e. pushover curve) at the top of the structure. The resulting pushover curves are presented in Fig. 7. It has been found that several analysis results such as the bending moment and shear force at the base, the force-strain curves, and the moment-curvature curves show only a small difference for the two force distributions [6].

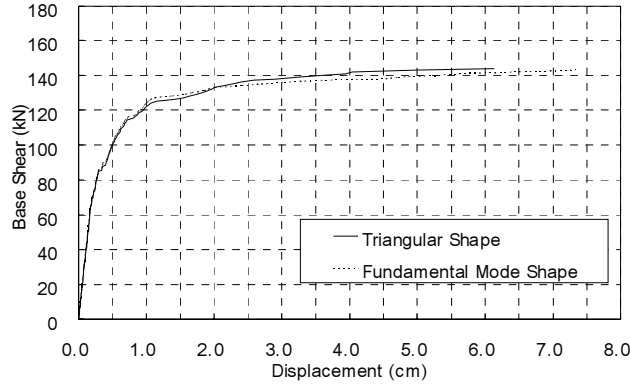


**Fig. 7. Force-displacement curve**

#### Displacement coefficient method (DCM)

The target displacement, which represents the expected maximum displacement of the structure for the earthquake load, is calculated using:

$$\delta_t = C_0 C_1 C_2 C_3 S_a (T_e / 2\pi)^2 \quad (2)$$

where  $C_0$  is the modification factor to relate spectral displacement of an equivalent single degree of freedom system to the roof displacement of the building;  $C_1$  is the modification factor to relate expected maximum inelastic displacements to displacements calculated for linear elastic response;  $C_2$  is the modification factor to represent the effect of pinched hysteretic shape, stiffness degradation and strength deterioration on maximum displacement response;  $C_3$  is the modification factor to represent increased displacements due to dynamic P- $\Delta$  effects;  $S_a$  is the response spectrum acceleration at the effective fundamental period and damping ratio (5% in this study) of the building in the direction under consideration; and  $T_e$  is the effective fundamental period of the building in the direction under consideration. The details of the method can be found in FEMA 356 [5].

In this study,  $C_0$  was set equal to  $PF1 * \phi_{1,roof}$  (in this case, 1.406) where PF1 is the first modal participation factor and  $\phi_{1,roof}$  is the amplitude of the fundamental mode at roof. The modification factors,  $C_2$  and  $C_3$ , were set to 1.  $C_1$  was set to 1.052, 1.0, 1.0, 1.435, 1.349, and 1.349 for Runs 1, 2, 3, 4, 4-5, and 5, respectively, according to the FEMA 356 procedures.

#### Capacity spectrum method (CSM)

The capacity spectrum method was developed by Freeman [7, 8]. This method uses the intersection of the capacity curve from a pushover analysis and a response spectrum curve from earthquake acceleration records to estimate the maximum displacement. It consists of the following steps [9]:

1. Develop the relationship between base shear,  $V_b$ , and top displacement,  $u$ , commonly known as the pushover curve.
2. Convert the pushover curve to a capacity diagram using the following equations:

$$A = V_b / M_1^* \quad (3)$$

$$D = \frac{u_N}{\Gamma_1 \phi_{N1}} \quad (4)$$

where

$$M_1^* = \frac{\left( \sum_{j=1}^N m_j \phi_{j1} \right)^2}{\sum_{j=1}^N m_j \phi_{j1}^2}; \quad (5)$$

$$\Gamma_1 = \frac{\sum_{j=1}^N m_j \phi_{j1}}{\sum_{j=1}^N m_j \phi_{j1}^2}; \quad (6)$$

$m_j$  is the lumped mass at the  $j^{\text{th}}$  floor level;  $\phi_{j1}$  is the  $j^{\text{th}}$  floor element of the fundamental mode  $\phi_1$ ;  $N$  is the number of floors; and  $M_1^*$  is the effective modal mass for the fundamental vibration mode.

3. Convert the elastic response spectrum from the standard pseudo-acceleration,  $A$ , versus natural period,  $T_n$ , format to the  $A$ - $D$  format, where  $D$  is the displacement spectrum ordinate.
4. Plot the demand diagram and capacity diagram together and determine the displacement demand. Involved in this step are dynamic analyses of a sequence of equivalent linear systems with successively updated values of the natural vibration period,  $T_{eq}$ , and equivalent viscous damping,
5. Convert the displacement demand determined in Step 4 to global top displacement and individual component deformation and compare them to the limiting values for the specified performance goals.

In ATC-40, three procedures for identifying the performance point are presented. Among three procedures provided in ATC-40, Procedures A and B are adopted in the study. In Procedure B, two kinds of structural behavior types, A and B, were investigated. According to ATC-40, values for damping modification factor,  $\kappa$ , vary depending on structural behavior types A, B, and C (ref. Table 8-1 in ATC-40[4]). The structural behavior types presented in ATC-40 are shown in Table 3.

**Table 3. Structural behavior types (Table 8-4 in ATC-40[4])**

Shaking Duration	Essentially new building	Average existing building	Poor existing building
Short	Type A	Type B	Type C
Long	Type B	Type C	Type C

## RESULTS AND DISCUSSION

Numerical and experimental natural frequencies are presented in Table 4, where the experimental ones are obtained from low level random excitation. The first and the third mode correspond to the first and the second lateral modes, respectively, and the second mode represents the first vertical mode. The results indicate that the structural stiffness of the linear stick model is overestimated. Estimated and measured top (maximum) displacements and base shear forces are summarized in Tables 5 and 6, respectively. Also given in the tables are the nonlinear time history analysis results by RCAHEST, where the Rayleigh damping corresponding to modal damping of 2% is used. In the tables, the responses estimated by the CSM are those from Procedure B for structural behavior types A and B (PB-TA and PB-TB), and from Procedure A for structural behavior type A (PA-TA). The base shear forces by experiment are calculated from measured accelerations of the structure and the corresponding masses. The tables show that the DCM gives the highest results and the CSM for structural behavior type A yields the lowest ones. It also can be found that the similar results are obtained from Procedures A and B of the CSM. It is noted that CSM Procedure A does not give converged responses for Run 1. In the tables, it can be seen that the top relative displacements by the DCM are in good agreement with the test results except for Runs 4 and 5 but the base shear forces do not match well with the test results. In the CSM Procedure, however, significant discrepancies between the analysis and the test results are observed in the top relative displacements as well as the base shear forces. In Run 2, where the responses seem to be in a linear range, the responses by all approaches are comparable to the test results. Further investigation and studies are needed on the analysis procedures and results in the displacement-based approaches, experimental data, etc. in the future. Further analysis is also needed utilizing more near- and far- field earthquake ground motions for grasping the effectiveness of the displacement-based approach for those earthquake ground motions.

**Table 4. Measured and estimated natural frequencies of the structure (Hz)**

	Mode 1	Mode 2	Mode 3
Experiment	7.2	28.1	31.1
Linear stick model	8.2	23.3	40.1
FE shell model	7.6	22.6	33.6

**Table 5. Comparison of the top displacement**

		Top Displacement (mm)					
		Run 1	Run 2	Run 3	Run 4	Run 4-5	Run 5
Experiment		7.00	1.54	13.20	13.4	13.4	43.3
Linear Analysis	Response Spectrum	4.62	1.81	13.37	2.68	11.4	20.0
Nonlinear Analysis	DCM	6.76	1.85	14.50	4.05	10.6	18.6
	CSM (PB-TA)*	2.91	1.69	6.96	4.92	6.05	23.3
	CSM (PB-TB)	3.22	1.69	8.15	8.01	6.96	28.7
	CSM (PA-TA)	2.7-3.5**	1.70	7.35	4.78	6.33	21.1
Time History		6.20	2.20	11.50	4.27	14.7	36.0

\* PB-TA : Procedure B/Type A; PB-TB : Procedure B/Type B; PA-TA : Procedure A/Type A

\*\* Not converged.

**Table 6. Comparison of the base shear force (for one wall)**

		Base Shear Force (kN)					
		Run 1	Run 2	Run 3	Run 4	Run 4-5	Run 5
Experiment		65.9	23.5	106.0	86.6	86.6	111.0
Linear Analysis	Response Spectrum	55.0	21.6	159.8	32.6	113.5	199.2
Nonlinear Analysis	DCM	56.8	33.0	64.3	45.5	63.0	65.6
	CSM (PB-TA)*	42.6	30.9	57.5	50.0	55.0	67.0
	CSM (PB-TB)	43.2	30.9	58.5	58.5	57.5	68.0
	CSM (PA-TA)	41-44**	31.0	58.0	49.4	55.0	66.5
	Time History	69.8	38.9	195.0	40.8	69.8	136.0

\* PB-TA : Procedure B/Type A; PB-TB : Procedure B/Type B; PA-TA : Procedure A/Type A

\*\* Not converged.

The comparisons of the relative top displacements from the nonlinear time history analysis by RCHHEST with the measured displacements can be seen in Fig. 8. The figure and Tables 5 and 6 show that most of nonlinear time history analysis results are in good agreement with test results except for Run 4. The largest maximum base shear force for Run 3 in Table 6 is due to a single instantaneous spike of a structural acceleration time history. Note that the analysis for Run 4-5, scaled down from Run 5 input motion, gives comparative results with the test results.

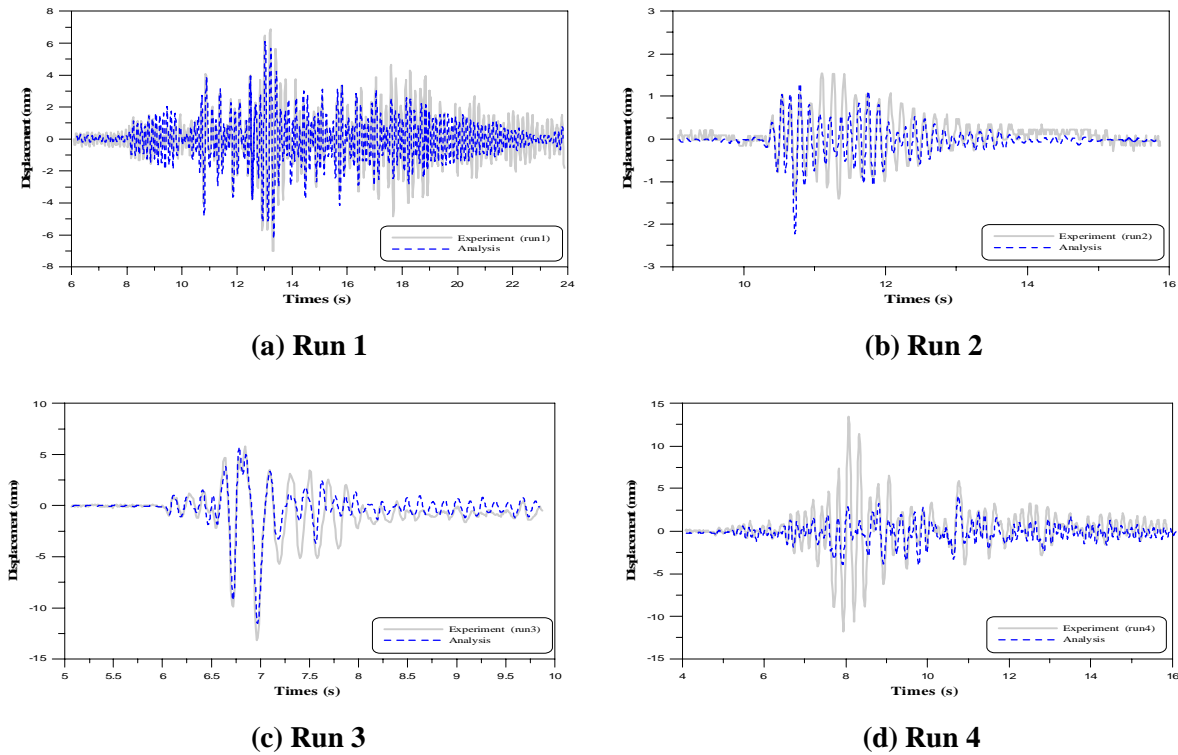
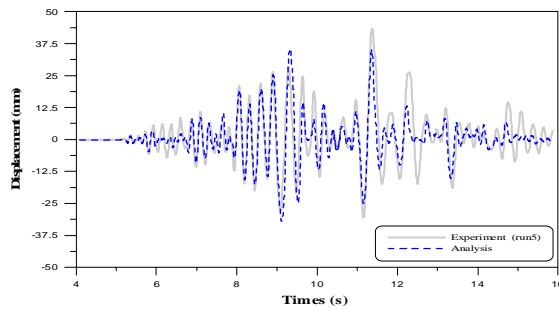
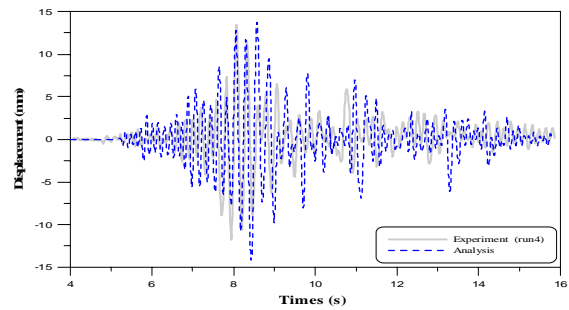


**Fig. 8. Comparison of relative top displacements**



(e) Run 5



(f) Run 4-5

**Fig. 8. (continued) Comparison of relative top displacements**

### ACKNOWLEDGEMENTS

Funding for this effort was sponsored by the IAEA, under grant number 12145/R0, the Ministry of Science and Technology (MOST) of Korea, and the Korea Institute of Nuclear Safety (KINS).

### REFERENCES

1. Combesure D. "IAEA CRP-NFE Camus benchmark: experimental results and specifications to the participants." IAEA, 2002.
2. SAP2000®, "User's Manual." Computers and Structures, USA, 1998.
3. Kim TH and Shin HM. "Analytical approach to evaluate the inelastic behavior of reinforced concrete structures under seismic loads." Korean Journal of Earthquake Engineering, 2001, 5(2): 113-124.
4. Applied Technology Council (ATC). "Seismic evaluation and retrofit of concrete buildings." SSC96-01: ATC-40, Redwood City, CA, USA, 1996.
5. Federal Emergency Management Agency (FEMA). "Prestandard and commentary for the seismic rehabilitation of buildings." FEMA-356, Washington, D.C., USA, 2000.
6. Hyun C-H, et al. "Safety significance of near field earthquakes / assessment of near field earthquake effects." KINS/GR-262, KINS, 2003.
7. Freeman SA, Nicoletti JP, and Tyrell JV. "Evaluations of existing buildings for seismic risk – a case study of Puget Sound Naval Shipyard, Bremerton, Washington." Proceedings of 1st US National Conference on Earthquake Engineering, EERI, Berkeley, USA, 1975, 113-122.
8. Freeman SA. "Prediction of response of concrete buildings to severe earthquake motion." Publication SP-55, ACI, Detroit, USA, 1978, 589-605.
9. Chopra AK and Goel RK. "Capacity-demand-diagram methods for estimating seismic deformation of inelastic structures: SDF systems." Report No. PEER-1999/02, Pacific earthquake engineering center, University of California, Berkeley, USA, 1999.